

# NORSAR

ROYAL NORWEGIAN COUNCIL FOR SCIENTIFIC AND INDUSTRIAL RESEARCH

NORSAR Scientific Report No. 1-85/86

## FINAL TECHNICAL SUMMARY

**1 April - 30 September 1985**

L. B. Loughran (ed.)

Kjeller, December 1985



APPROVED FOR PUBLIC RELEASE, DISTRIBUTION UNLIMITED

### VII.5 P-wave spectra from NORESS recordings

A number of earlier studies, some of which based on NORSAR data, have shown that high frequency signal propagation in Eurasia is very efficient, even at teleseismic distances. With the new NORESS installation in Norway, we now have the possibility to study both the spectral contents and spatial coherency of teleseismic phases at higher frequencies than before, since the NORESS SP system, which is based on 40 Hz sampling rate, effectively records signals of up to about 15 Hz frequency.

We have initiated a systematic study of the spectral characteristics of NORESS-recorded seismic phases, and in this paper we present some representative examples, together with brief comments summarizing the most important features. Five events of low and intermediate magnitude ( $m_b$  4.0-5.0) have been chosen, at least three of these are presumed underground explosions. The events are in the epicentral distance range 14-49 degrees. In Figs. VII.5.1 to VII.5.5 we show, for each event, NORESS single sensor and beam time domain traces as well as spectral plots of signal and noise. The beam has been steered to the event epicenter using plane-wave time delays, and is based on the subset of NORESS instruments comprising the center instrument and the C and D rings, i.e., 17 of the 25 NORESS SPZ channels. As discussed by Mykkeltveit et al (1985), this subset provides particularly efficient noise suppression in the band 1.5-3.0 Hz, and is better than the full array in this regard.

The noise spectra have been estimated using the indirect covariance method. We first estimate the correlation function by splitting a long data record into many windows, calculating a sample correlation function for each window, then averaging the sample correlation functions. Typically, we use 20 windows, each of which is 5 seconds long. Because the earth noise has such a

large dynamic range, we prewhiten it prior to estimating the correlation function with a low-order prediction-error filter. The spectrum is then estimated by windowing the correlation function with a 3-second Hamming window, then computing the Fourier transform. The spectral estimate obtained this way is compensated then for the effects of prewhitening and normalized to a 1-second window length.

Signal spectra have been estimated using the same technique, but with 4 overlapping windows, each of 7 seconds length. Start times of these windows are 3, 2, 1 and 0 seconds before signal onset, respectively. Thus we achieve a smoothing of the signal spectra while retaining compatibility with the noise spectra.

The NORESS digital recording system employs gain-ranged 16 bits data words, as described by Stokes (1982). While the overall dynamic range is as large as 120 dB, the actual resolution at any given gain level is considerably lower. Thus, quantization effects become significant for those portions of the spectra which are 70 dB or more below the spectral peak of a given signal, and this must be kept in mind when reviewing the spectra displayed in this subsection. The quantization effects are manifested in these plots as an oscillation in the spectral traces, which is apparent on some events at very high frequencies.

In the following, we briefly comment on the main features of the five events selected:

Event 1: 66.ON 40.8E, distance 14 deg, azimuth 55 deg,  $m_b=5.0$

The P wave is very complex, with significant high frequency energy, especially in the P coda. Much of the high frequency energy is lost on the beam, as seen both from the time domain plots and the spectra. There is significant SNR over the entire

frequency band shown, and in fact it appears likely that there would be significant energy also above 15-20 Hz for this event. However, the largest SNR is found in the 2-8 Hz band. This event is in the regional distance range, and has large Sn and Lg phases recorded by NORESS.

Event 2: 46.8N, 48.1E, distance 25 deg, azimuth 107 deg,  $m_b=5.0$

The P wave is complex also for this event, due to multiple onsets from different upper mantle P phases. The signal has a clear spectral density peak at 2 Hz, and the spectral density drops much more rapidly with increasing frequency than for Event 1. There appears to be no significant SNR above 12 Hz frequency, even though the quantization noise makes a definite conclusion difficult. Beam signal loss is negligible up to 6 Hz in this case.

Event 3: 49.9N 78.1E, distance 38 deg, azimuth 75 deg,  $m_b=4.9$

This event is characterized by a very clear, impulsive P signal. A sharp spectral peak is seen at 2 Hz for the signal, and there is significant SNR out to at least 15 Hz. Beam signal loss is negligible up to 6 Hz. Note the pronounced noise suppression on the beam around 2 Hz (associated with the choice of subgeometry discussed before); this feature, which here is particularly visible, can also be identified on the other figures by close inspection.

Event 4: Central Asia (no NEIS location, distance  $\sim 40$  deg, azimuth  $\sim 80$  deg,  $m_b=4.0$

This is a low magnitude event from the same general area as Event 3, and many of the same comments apply. The recordings illustrate in particular the large SNR gain on the beam, especially around 2 Hz, and it is noteworthy that even for an event

at such low magnitude, a significant SNR can be found on the beam up to around 10 Hz frequency.

Event 5: 41.7N 88.4E, distance 49 deg, azimuth 76 deg,  $m_b=4.7$

This event has a clear, impulsive P phase recorded at NORESS. In contrast to previous event, the signal power around 2 Hz is much lower than the spectral maximum, thus the best SNR occurs at 4 Hz frequency. Again, the beam has significant SNR up to about 10 Hz.

In conclusion, the studies of these and other events have shown that P phases from intermediate and low magnitude Eurasian events very often contain signal energy well above the noise level up to at least 10 Hz frequency. However, for teleseismic events, the SNR on the beam is usually best at frequencies below 4 Hz; thus for teleseismic event detection purposes, a set of bandpass filters covering the range 1-5 Hz would be expected to give the best performance. At the high frequency end, there is clearly a potential for additional SNR gains through beamforming based on array subgeometries involving only the inner rings, and this will be the topic of a separate investigation.

We emphasize that these results are preliminary, and we plan to continue our research on this topic.

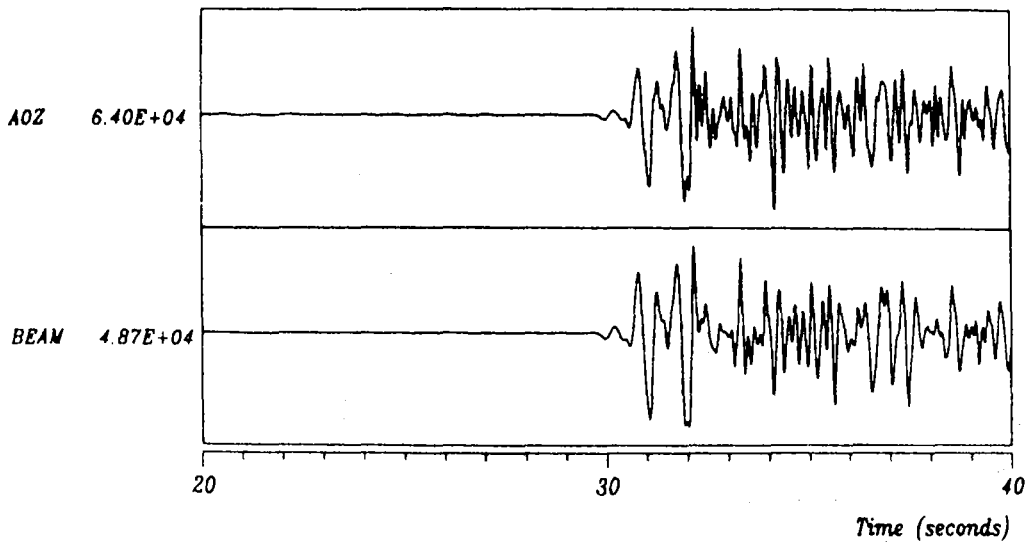
T. Kväerna  
F. Ringdal

References

Mykkeltveit, S., D.B. Harris & T. Kvarna (1985): Preliminary evaluation of the event detection and location capability of the small aperture NORESS array, NORSAR Semiannual Technical Summary, 1 Oct 84 - 31 Mar 85, NORSAR, Kjeller, Norway.

Stokes, P.A. (1982): The National Seismic Station, Sandia Report SAND81-2134.

PST 85 199 21 17 45 69



07/18/85 21.15.00

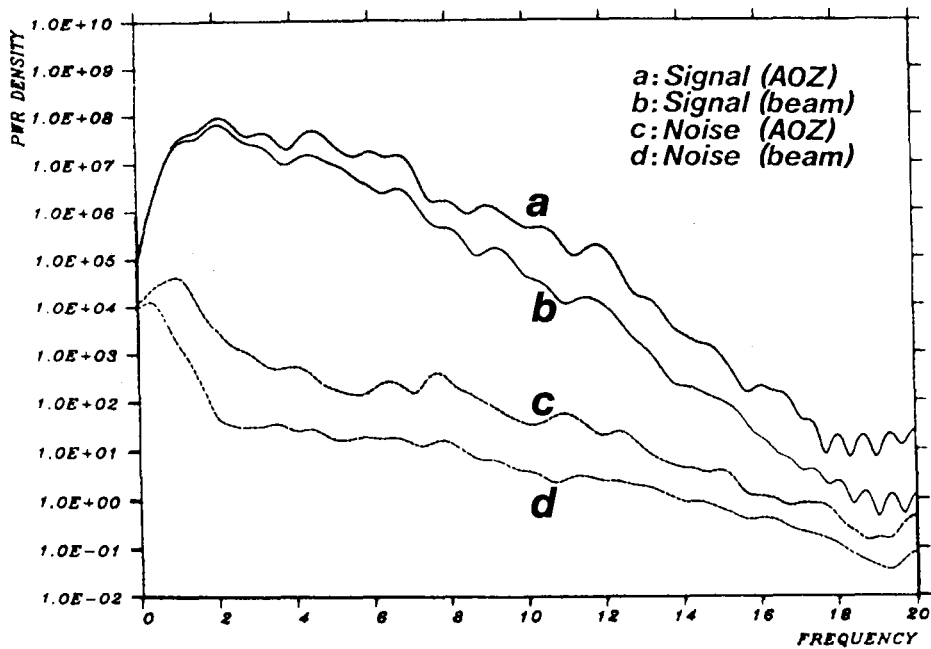
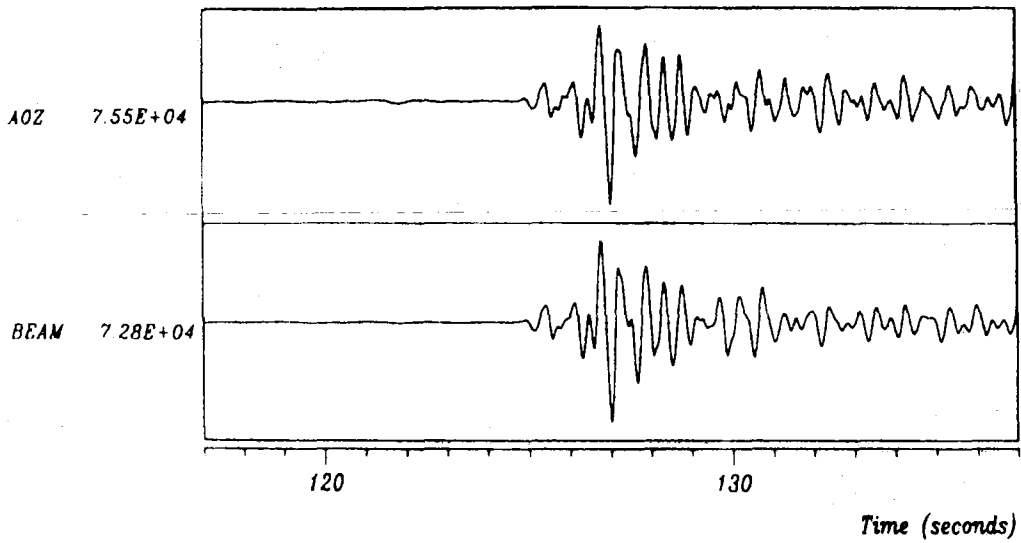


Fig. VII 5.1 The top part of the figure shows NORESS single sensor trace (instrument A0Z) and NORESS steered beam (employing the 17 seismometers A0, C1-7, D1-9) for Event 1 described in the text. The lower part of the figure shows power density spectra for (a) signal (A0Z), (b) signal (beam), (c) noise (A0Z) and (d) noise (beam). Tick marks on the vertical axis correspond to 10 dB power increments. The spectra have not been corrected for system response.

PST 301 06 03 20 80



10/27/84 06.00.00

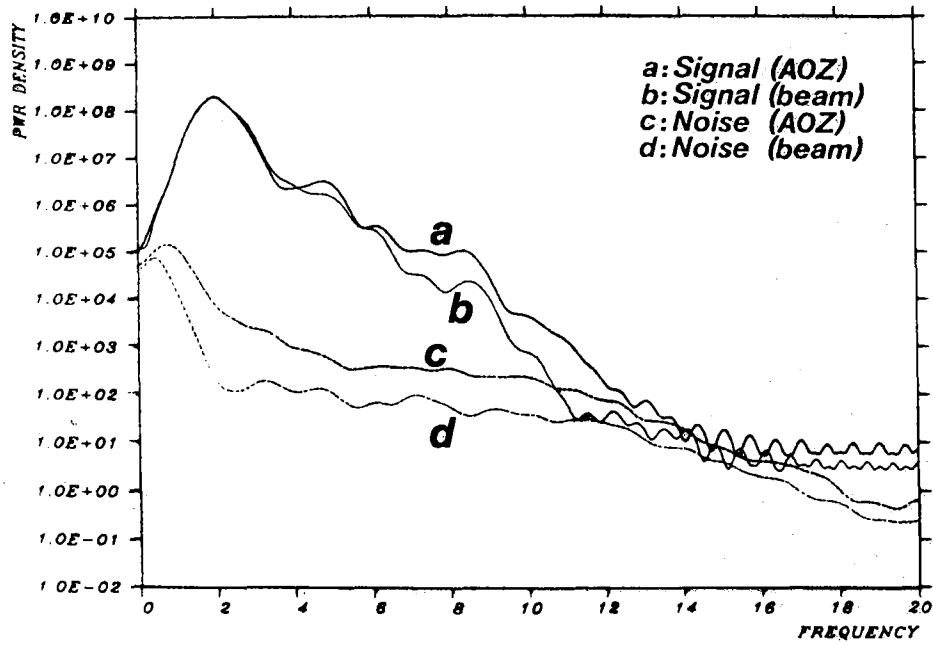
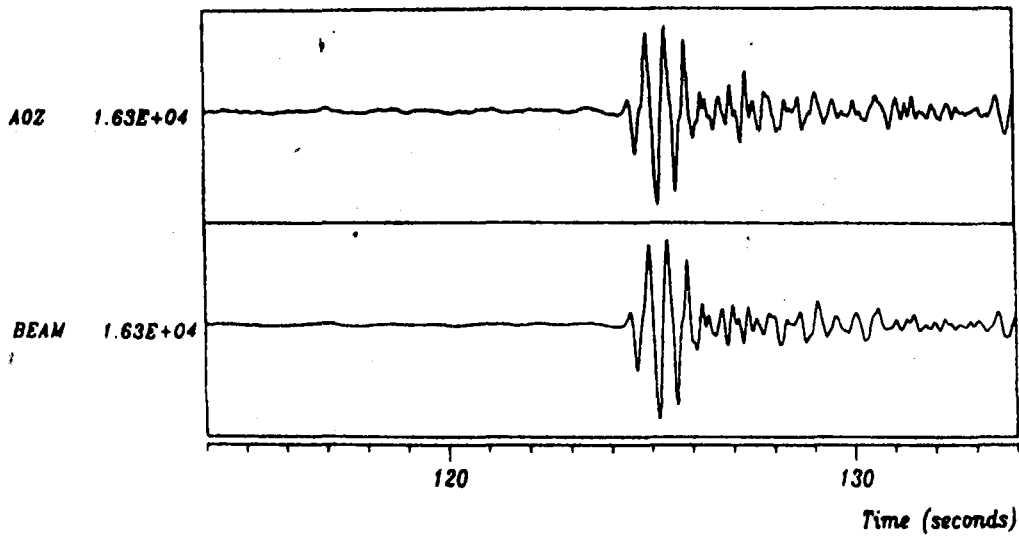


Fig. VII.5.2 Same as Fig. VII.5.1, but for Event 2 described in the text.



PST 85 206 03 16 20 74



07/25/85 03.11.00

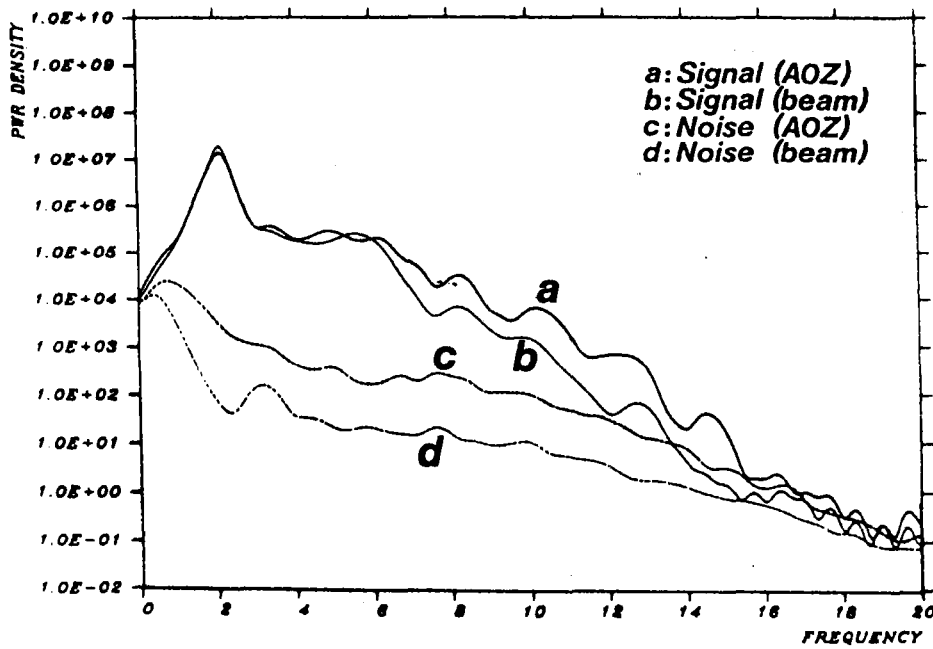


Fig. VII.5.3 Same as Fig. VII.5.1, but for Event 3 described in the text.

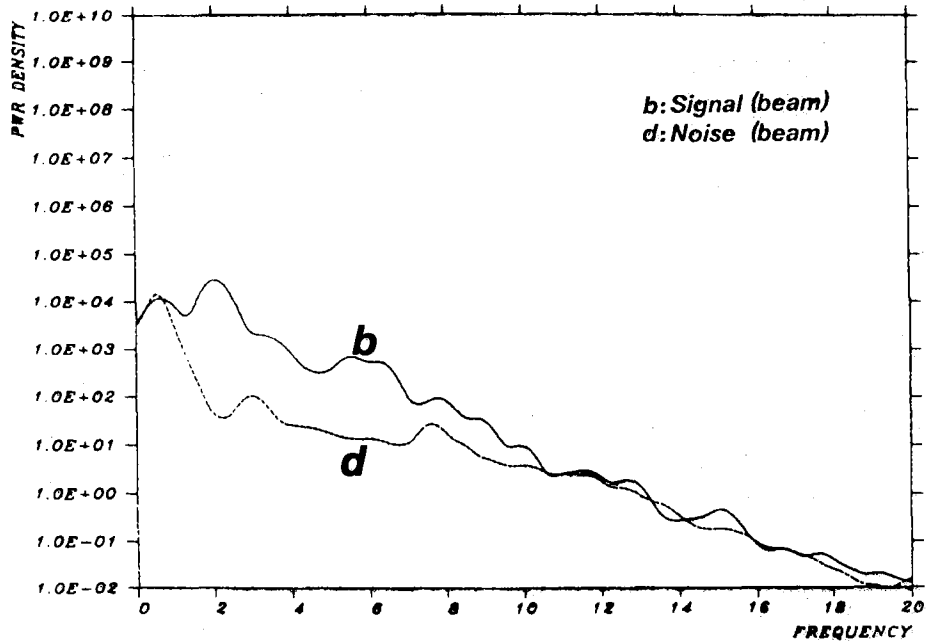
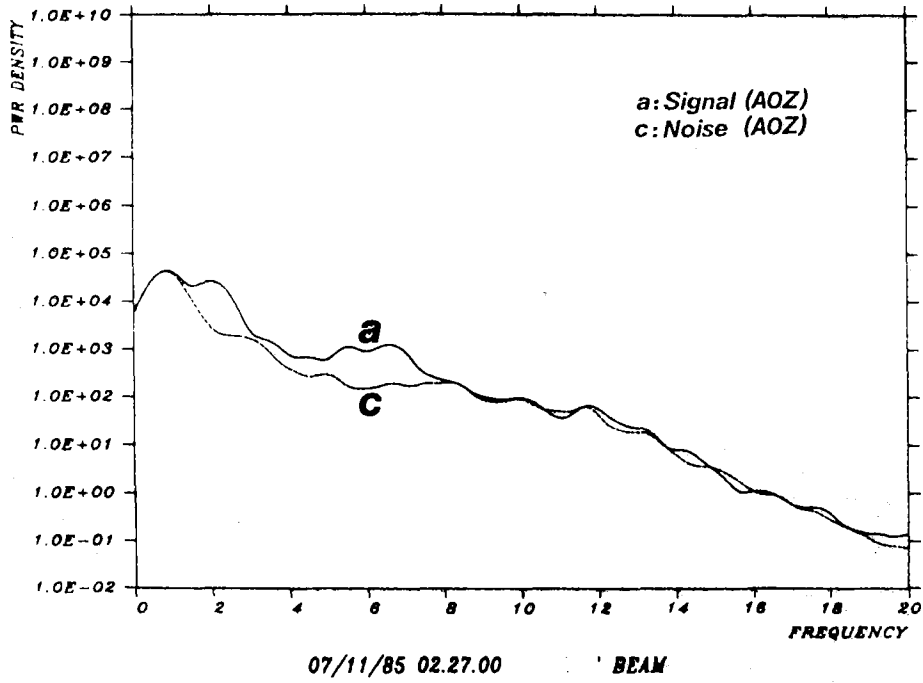
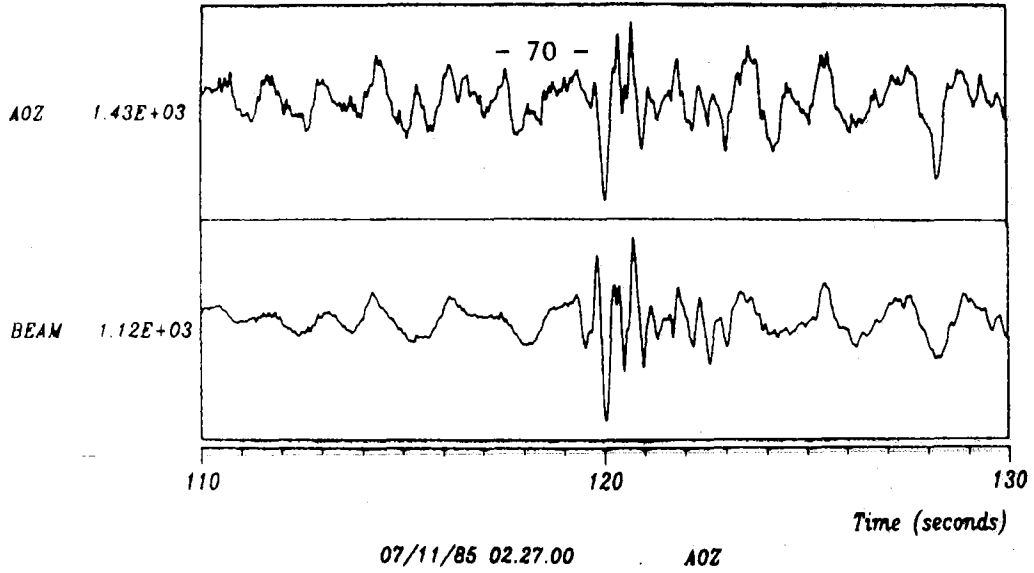


Fig. VII.5.4 Same as Fig. VII.5.1, but for Event 4 described in the text.

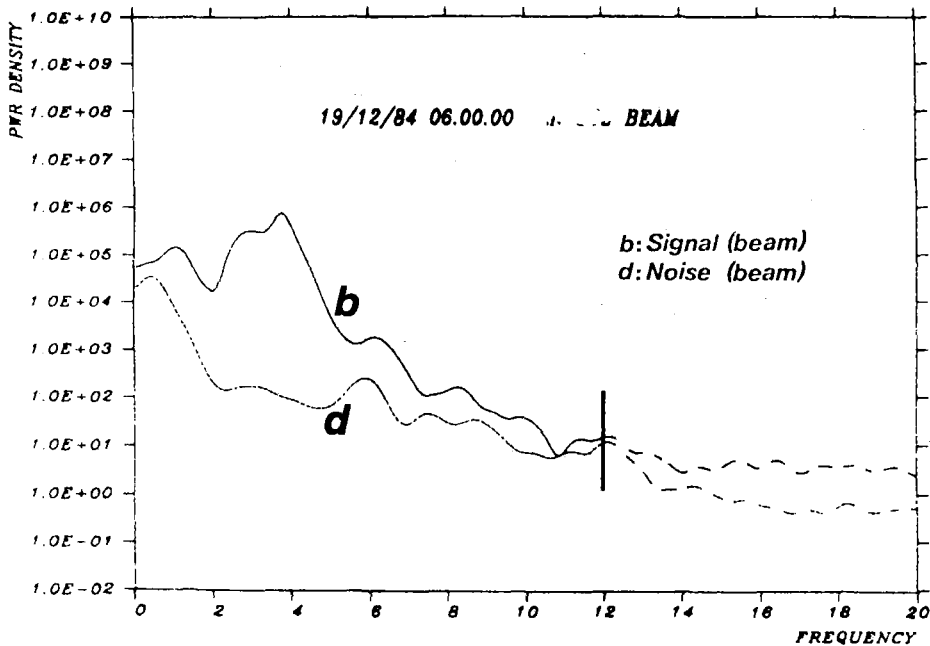
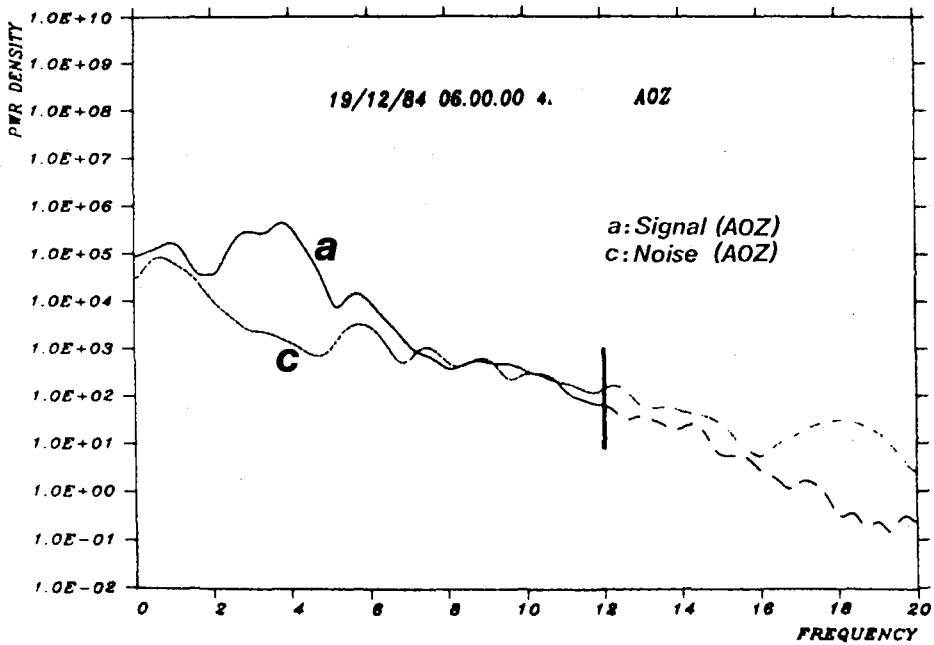
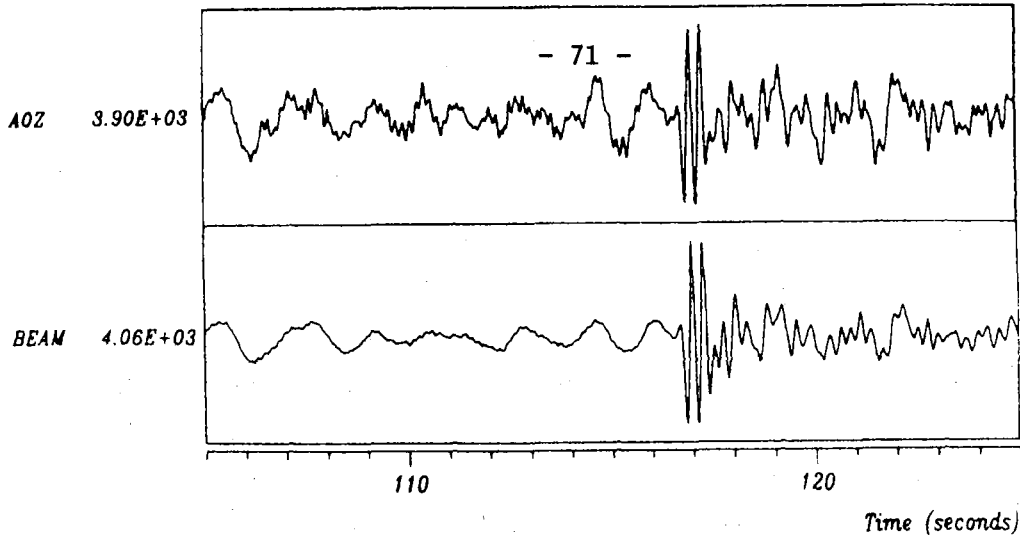


Fig. VII.5.5 Same as Fig. VII.5.1, but for Event 5 described in the text. Due to data problems, the spectra for this event are based on shorter time windows than Events 1-4, and the spectral estimates beyond 12 Hz are uncertain.